The Effect of Omega Phase on the Mechanical Properties of Titanium Alloys

J. C. WILLIAMS, B. S. HICKMAN, AND H. L. MARCUS

The effect of the precipitation of the metastable ω phase on the tensile properties of β-phase titanium alloys has been studied. The volume fraction of ω phase was varied by controlling the heat treatment temperature and the alloy content. It is shown that provided the volume of ω phase is less than 0.6, significant increases in yield strength can be obtained while retaining reasonable ductility. Higher volume fractions results in complete macroscopic embrittlement, but fracture still occurs by microvoid coalescence. Thin film microscopy of deformed samples shows that dislocations bypass the omega particles. The results are discussed in relation to current theories of deformation and fracture of two-phase alloys.

DURING the early stages of β-phase titanium alloy development, an unexpected embrittlement was encountered during aging. Investigation of this embrittlement was responsible for the discovery of a transition precipitate known as the ω phase.[1] Subsequent studies using X-ray diffraction and, more recently, transmission electron microscopy and quantitative X-ray diffraction techniques have successfully defined most of the features of the $\beta \rightarrow \beta + \omega$ transformations.[2-6] These studies have shown that the ω-phase forms as a uniform distribution of relatively small, coherent particles, the volume fraction of which can reach 0.9 in some alloys. Much more limited information is available regarding the mechanism of embrittlement; the only notable discussion is due to Silcock[7] who suggested that the precipitates on only one of the four variants of the orientation relationship were suitably oriented for slip. Recently, electron fractography studies[8] of $\beta + \omega$ structures have shown that macroscopically brittle tensile specimens exhibit a microvoid coalescence fracture mode; the void size decreases with increasing aging time, *i.e.*, with increasing ω-phase volume fraction. This suggests that the embrittlement results from a continuous loss of ductility, rather than a change in fracture mode, such as is associated with temper embrittlement in steel.

In the current study we have examined the possibility of using a controlled volume fraction of the ω phase as a precipitation hardening dispersion. Earlier work[2-6] has shown that the volume fraction can be controlled by:

i) varying the aging temperature,

ii) varying the solute content of the β phase either by changing the initial alloy content or by solution treating in the $\alpha + \beta$ phase field to give an enriched β phase,

iii) by ternary additions of such elements as Al, Sn, and O.

J. C. WILLIAMS is Group Leader, Physical Metallurgy Group, North American Rockwell Science Center, Thousand Oaks, Calif. B. S. HICKMAN, formerly with North American Rockwell Science Center, is now Director of Research and Development, Australian Consolidated Industries, Waterloo, N.S.W., Australia. H. L. MARCUS is Group Leader, Fracture & Metal Physics Group, North American Rockwell Science Center.

Manuscript submitted August 20, 1970.

We have used all three of these methods to control the ω-phase volume fraction and tensile properties have been measured as a function of ω phase volume fraction. We have also attempted to define the mechanism of ω-phase embrittlement.

EXPERIMENTAL TECHNIQUES

1) Materials

Three experimental alloys, Ti-6 at. pct Mo, Ti-10 at. pct Mo, and Ti-25 at. pct V, were prepared by standard arc melting techniques from crystal bar titanium. The melted ingots were homogenized and then cold rolled to 0.030 in. sheet. In addition, two commercial alloys, Ti-8 pct Mn obtained from TMCA and Ti-11.5 pct Mo-4.5 pct Sn-6 pct Zr (known as Beta-III) obtained from Colt Industries as 0.030 in. sheet, were used. Tensile specimens with a 2 in. gage length were cut from the sheet.

All solution heat treatments were carried out in a vacuum furnace and the specimens were quenched by dropping them into a jet of helium gas precooled to liquid nitrogen temperature. Aging treatments were also carried out in a vacuum.

Tensile testing was done on an Instron machine at a strain rate of 3×10^{-4} per sec at room temperature. All reported results are the average of tests of two or more specimens with the same heat treatment. Samples for transmission electron microscopy were prepared using the technique described by Blackburn and Williams.[9] ω-phase volume fractions were measured by an X-ray technique described earlier by Hickman.[2]

RESULTS

a) Ti-Mo Alloy

The Ti-6 at. pct Mo alloy was quenched from above the β transus, aged in the range 350 to 450°C and tested. The ω-phase volume fraction was determined to be 0.8 to 0.9 in the aged alloys; however, these samples failed prior to macroscopic yielding in all cases and this alloy was thus abandoned.

The Ti-10 at. pct Mo alloy quenched from above the β transus and aged exhibits measurable ductility; a series of heat treatment times and temperatures have

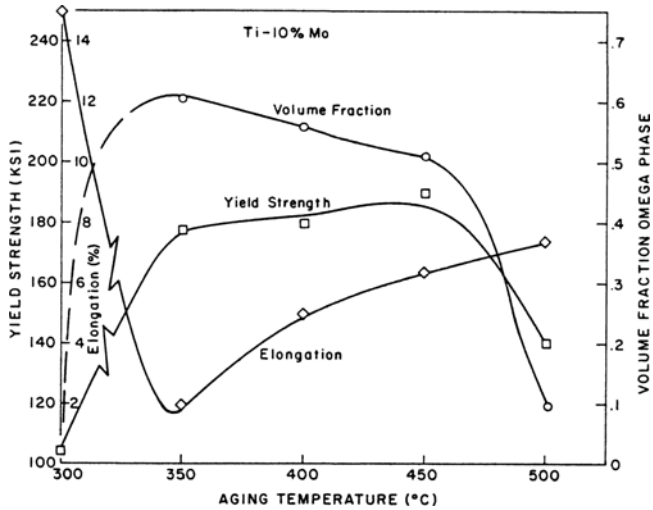

Fig. 1—Yield stress variations as a function of aging temperature for a Ti-10 at. pct Mo alloy. The aging times at each temperature were long enough to allow the metastable equilibrium volume fraction of ω phase to be formed. The elongation scale is shown inside the graph along the left-hand ordinate. Data points on left-hand ordinate represent as-quenched condition.

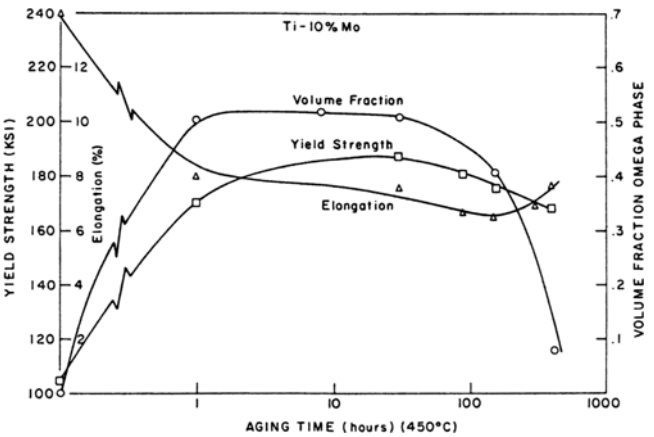

Fig. 2—Yield stress variations as a function of aging time at 450°C for the Ti-10 at. pct Mo alloy. Between 1 and 100 hr the yield strength and elongation can be seen to change at essentially constant ω-phase volume fraction. Data points on left-hand ordinate represent as-quenched condition.

been examined in this alloy. The ω-phase volume fraction in this material is ~0.5 to 0.6 maximum. Fig. 1 shows the variations in yield strength, elongation and ω-phase volume fraction as a function of aging temperature in this material. The aging times at each temperature (24 hr at 350°, 8 hr at 400°, and 2 hr at 450°C) were sufficient to produce the maximum volume fraction of ω phase attainable at each of these temperatures. Fig. 1 shows that the yield strength of the Ti-10 at. pct Mo alloy can be increased ~90 pct while maintaining elongations of 5 to 6 pct. No ω phase is formed in this alloy at aging temperatures $\geq$ 500°C, since in this temperature range the equilibrium α-phase forms directly. When the α phase is formed, the yield stress decreases in comparison to the samples which contain ω-phase, as shown in Fig. 1. Fig. 2 illustrates the influence of aging time at 450°C; the marked increase of yield stress which accompanies ω-phase formation is also apparent in this figure. At this temperature, aging times of $\gtrsim$100 hr result in α-phase formation which again leads to decrease in yield stress with attendant increases in elongation. In all heat treatment conditions the work hardening rate of the Ti-10 at. pct Mo alloy was low, thus the difference between ultimate and yield strengths was small. Electron fractography showed that failure occurred by dimple rupture in all cases, the dimple size decreasing with increasing aging time as shown in Figs. 3(*a*) through (*c*).

b) Ti-V Alloy

A series of specimens of a Ti-25 at. pct V alloy were quenched from the β-phase field and aged at temperatures of 300°, 350°, and 400°C for times long enough to produce the maximum volume fraction of ω phase at each temperature. These results are shown in Fig. 4 from which can be seen the rather large changes in yield stress that also accompany ω-phase formation in this alloy. The as-quenched yield strength of this alloy is lower than that of the Ti-10 at. pct Mo alloy and the observed strength increases were smaller. The observed maximum strength increases were still substantial (50 to 55 pct), however, and acceptable elongation values were still obtained. The work-hardening rate in the Ti-25 at. pct V alloy was much greater than the Ti-10 at. pct Mo, resulting in a larger difference betweeen ultimate and yield strengths.

The Ti-25 at. pct V alloy was also solution treated in the $\alpha + \beta$ phase field at 625°C to enrich the β phase in vanadium. Testing of the material in the quenched and in the quenched and aged conditions showed no increase in strength after aging, although X-ray diffraction measurements showed that the aged material contained ~0.25 to 0.30 volume fraction ω phase in the parent β phase.

c) Ti-Mn Alloy

The β phase composition of a Ti-8 wt pct Mn alloy was varied by solution treatment above the β transus (775°) and at 700° and 650°C, which are below the transus in the $\alpha + \beta$ (enriched) region and result in β phase containing 11 and 15 wt pct Mn, respectively. Aging the 775°C quenched material resulted in complete embrittlement, the specimens failed prior to macroscopic yielding, frequently in the grip section. The ω-phase volume fraction in these samples was 0.8 to 0.9. The 650°C quenched material showed no aging response, but electron microscopy and X-ray diffraction observations on this material showed that ω phase was present, the volume fraction being $\lesssim$0.25. The 700°C quenched material showed significant hardening on aging, as shown by the data in Table I. As in the Ti-25 at. pct V alloy, this material exhibited a relatively high work-hardening rate as evidenced by the spread between the the yield and ultimate tensile strengths.

d) Ti-11.5Mo-4.5Sn-6Zr Alloy (Beta-III)

This alloy is essentially a commercial variation of the Ti-Mo alloys, the tin and zirconium being added to

retard ω-phase formation. This material was also solution treated above (750°C) and below the β transus (700° and 650°C) to vary the initial composition of the β phase. As was observed in the Ti-8 wt pct Mn alloy, the 750°C quenched material was completely embrittled after aging at 350° of 400°C, but aging at 450°C produced a 95 ksi increase in yield stress with the retention of ~4 pct elongation, as shown in Fig. 5. These results and the remaining results for β-III are shown in Table II. The aging response of the 650°C solution treated material was insignificantly small, although X-ray diffraction measurements showed that the ω-phase volume fraction in these samples was 0.15 to 0.20. Aging the 700°C solution treated material showed relatively small yield stress increases due to ω phase with an attendant decrease in ductility. As mentioned earlier, the 750°C solution treated material aged at 450°C exhibited a yield stress of 195 ksi with 4 pct

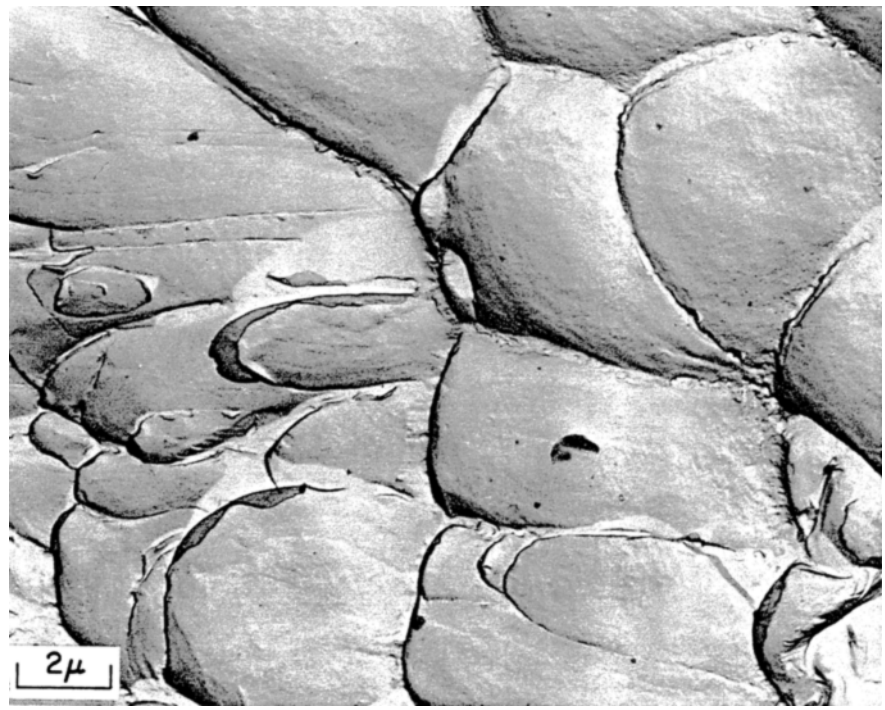

(*a*)

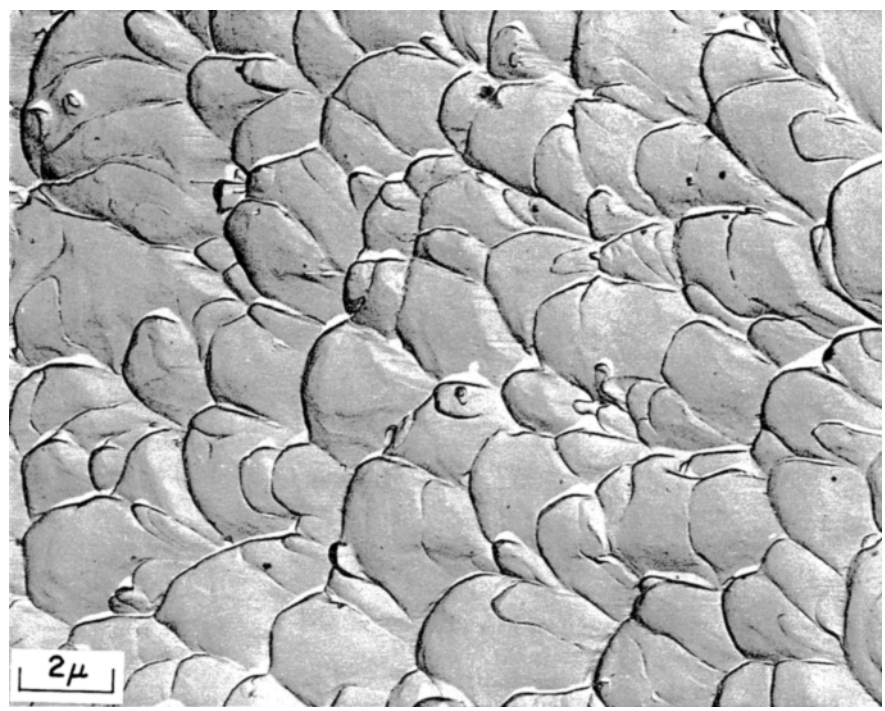

(*b*)

Fig. 3—Two stage replica electron fractographs of Ti-10 at. pct Mo tensile specimens showing the variation in dimple size as a function of aging time at 350°C: (*a*) aged 1 hr; (*b*) aged 24 hr; (*c*) aged 100 hr.

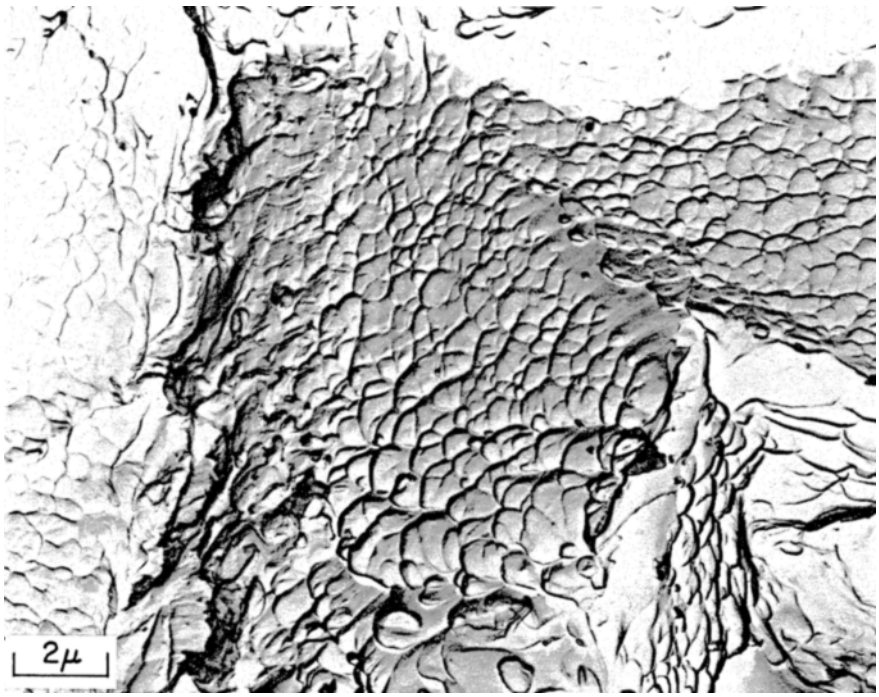

(c)

Fig. 3—continued

Table I. Tensile Data on Ti-Mn Alloys

Solution Treatment Temperature, °C	Aging Temp, °C	Time, hr	Y.S., ksi	U.T.S., ksi	Elongation, Pct	Volume Fraction ω Phase
650	As-Q		129	143.5	25	Nil
	350	24	125	142	24	30
	400	8	126	147	23	25
700	As-Q		139	148	23	Nil
	350	24	156	202	4.5	65
	400	8	170	198	4.0	60
775	As-Q		160	166	9.5	30
	300	100	all specimens failed in brittle fashion before macroscopic yielding			90
	350	24				85
		100				
	400	8				80

elongation; the ω-phase volume fraction in this condition is ~0.50 to 0.60.

e) Deformation and Fracture Behavior of ω-Phase Strengthened Alloys

We have prepared thin foils from the gage sections of various tensile specimens tested in this study in an attempt to examine the deformation behavior of β + ω mixtures. Two experimental difficulties have been encountered. Firstly, in the completely brittle specimens the ω-phase particle density is so great that dislocations in the β matrix are not discernible due to the overlapping images of ω particles and we have obtained no information from these alloys. Secondly, in those alloys which had measurable ductility the ω phase particles were quite small, usually < 100Å in maximum dimension and this rendered observation of

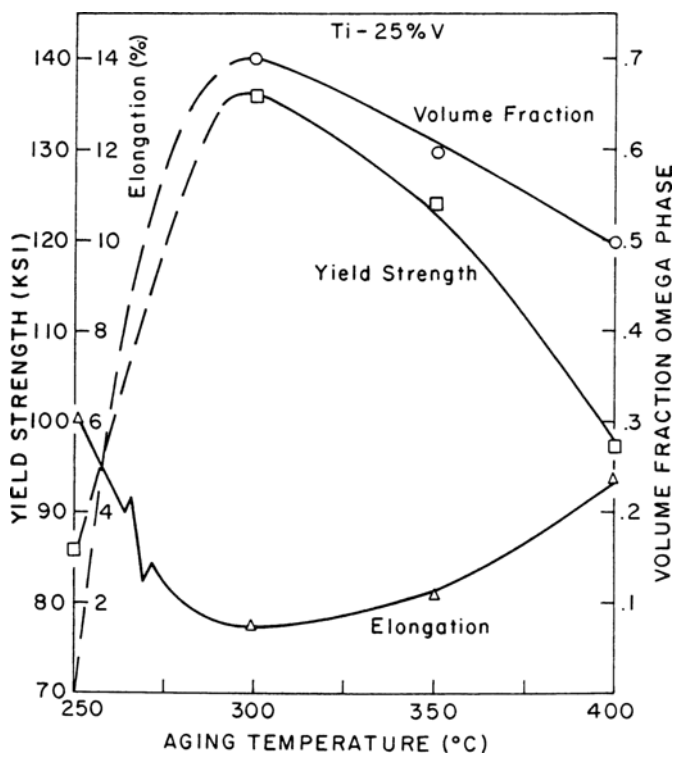

Fig. 4—Yield stress variations as a function of aging temperature in a Ti-25 at. pct V alloy. As in Fig. 1, aging times were long enough to produce the metastable equilibrium volumes fraction of ω phase.

the nature of the interaction between dislocations and the ω-phase particles difficult, at best. In these alloys no evidence for particle shearing has been obtained

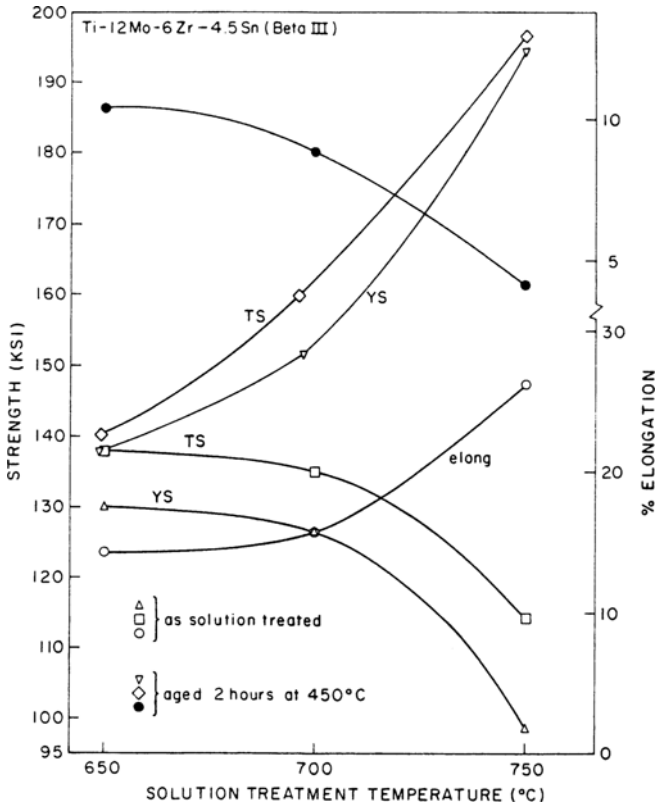

Fig. 5—Yield stress variations of the commercial metastable β-phase alloy Ti-11.5Mo-6Zr-4.5Sn (β-III) as a function of solution treatment temperature. The lower set of curves are for the "as-quenched" material, whereas the upper set of curves are for the material after quenching and aging 2 hr at 450°C.

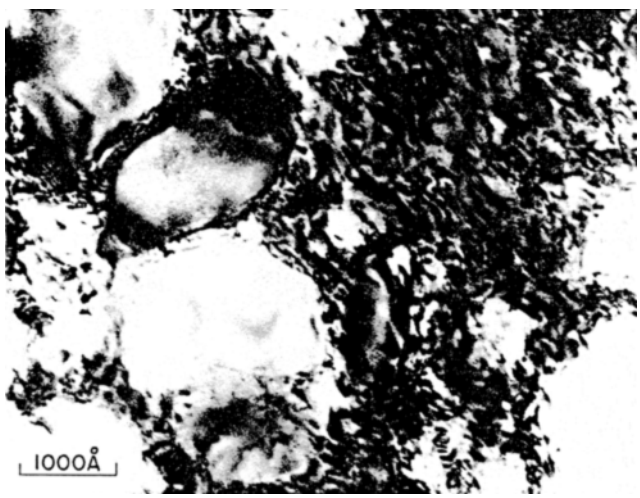

(*a*)

Fig. 6—Thin foil micrographs of a Ti-20 wt pct V-10 wt pct Zr alloy quenched from 950°C, aged 20 hr at 400°C and deformed ~ 5 pct at room temperature. (*a*) Showing the very high dislocation density in the matrix with no dislocations in the ω-phase particles (labeled). (*b*) Showing the inhomogeneous nature of the deformation, even on a highly localized scale. (*c*) Thin foil micrograph of β-III, quenched from 850°C and aged 5 min at 450°C, showing the bypassing of particles and the formation of dislocation loops around some particles (arrows). Particles without dislocation loops around them can also be seen in the same area.

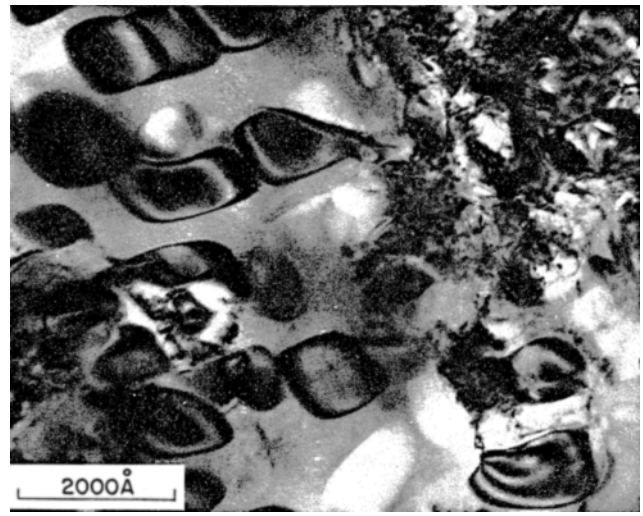

(*b*)

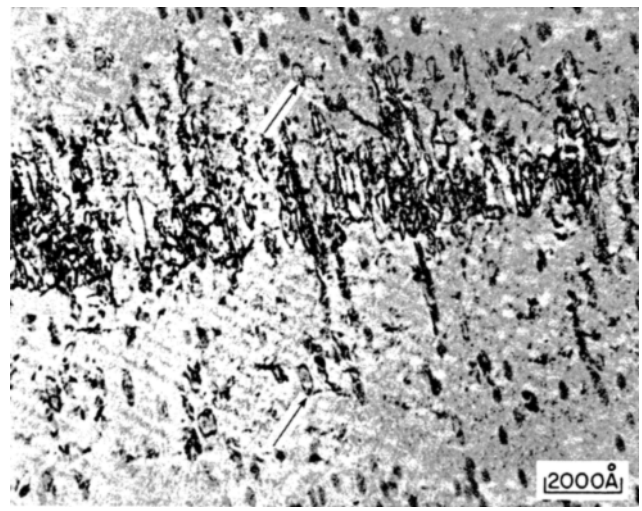

(*c*)

and the dislocations generally appear to stop at the particles or bend around them where this is possible. To more convincingly illustrate this point we have deformed a Ti-10 wt pct Zr-20 wt pct V alloy which contains larger (2000Å) ω-phase particles in combination with a smaller ω-phase volume fraction (~0.60) than has been observed in the other alloys. Tensile testing showed that hardening due to ω-phase also occurred in this alloy. From Figs. 6(*a*) through (*c*) it can be seen that the dislocations do not appear to penetrate the ω-phase particles and the result is an extremely high dislocation density in the β-phase matrix. The fracture surfaces of these and other samples have been examined by electron fractography and in all cases the mode of failure has been verified as microvoid coalescence or dimple rupture. There is good qualitative agreement between macroscopic ductility and dimple size, as shown in Figs. 3(*a*) through (*c*) for a Ti-10 at. pct Mo alloy. During the earlier stages of aging, large elongated features are often observed, as shown in Fig. 7. The origin of these features is not altogether clear, but they do appear to be generally associated with the β-grain boundaries. It is possible

Table II. β-III

Solution Treatment Temp	Aging Temp	Time, hr	Y.S., ksi	U.T.S., ksi	Elongation Pct	Volume Fraction ω Phase
650°C	As-Q		130	139	14	Nil
	350	24	138	140	9	–
	400	8	136	140	10	20
	450	2	139	145	10	15
700°C	As-Q		128	136	16	Nil
	350	24	155	160	5	45
	400	8	158	167	5	40
	450	2	148	158	8	35
750°C	As-Q		100	115	22	Nil
	350	24	Brittle			–
	400	8	Brittle			65
	450	2	195	198	4.5	60

that these features represent "shear bands" where the ω phase has been cut during deformation; such an explanation would account for their absence at longer aging times where the ω is not sheared during deformation.

DISCUSSION OF RESULTS

The data presented in this paper provide a basis for the qualitative understanding of the strengthening and embrittling effects of the ω phase. Thus far we have related the increase in yield stress during aging to the ω-phase volume fraction and have obtained reasonable agreement in all systems studied. However, closer examination of some of our results shows that the yield stress continues to increase after the ω-phase volume fraction has stabilized; this is best seen in Fig. 2. Hickman[2,3] has shown that the compositions of the β and ω phases continue to change after the maximum volume fraction is reached. The total increase in strength can be formally separated into a precipitation hardening component $\Delta\tau_p$ and component due to solid solution hardening of the matrix $\Delta\tau_s$. The ~15 ksi yield strength increase shown in Fig. 2 after the ω volume becomes constant is ascribed to matrix strengthening by molybdenum enrichment. The elastic misfit between the precipitate and matrix also increases during aging and it is possible that this also contributes to the observed 15 ksi increment. The limited solid solution strengthening data available for Ti-Mo alloys shows this strength increase is consistent with a matrix enrichment of ~6 wt pct, which is in reasonable agreement with the β-phase composition data of Hickman. Thus the strengthening can be accounted for on the basis of an increased $\Delta\tau_s$ and we shall not consider any changes in the elastic misfit in the remaining discussion.

A comparison of strengthening per vol pct ω-phase is shown in Fig. 8 for β-III and for Ti-V alloys. The β-III alloy behaves very similarly to Ti-Mo during aging since the zirconium and tin do not selectively partition to either the β or ω phases to the extent that molybdenum does. The more marked strengthening in β-III is ascribed to larger values of $\Delta\tau_s$ in Ti-Mo-type alloys, since solid solution strengthening data for Ti-V and Ti-Mo alloys shows that molybdenum is a more effective solid solution strengthening solute in the bcc β phase. Such comparisons must be approached with caution since the β-phase composition ranges pertinent to the current question of ω-phase strengthening overlap the compositions where bulk bcc samples deform by twinning,[5,10] whereas β + ω mixtures deform by slip. The comparisons we have made above only apply to compositions where the de-

Fig. 7—Two-stage replica electron fractograph of Ti-10 at. pct Mo tensile specimen quenched from 950°C showing large shear-like features which are characteristic of this intermediate aging condition.

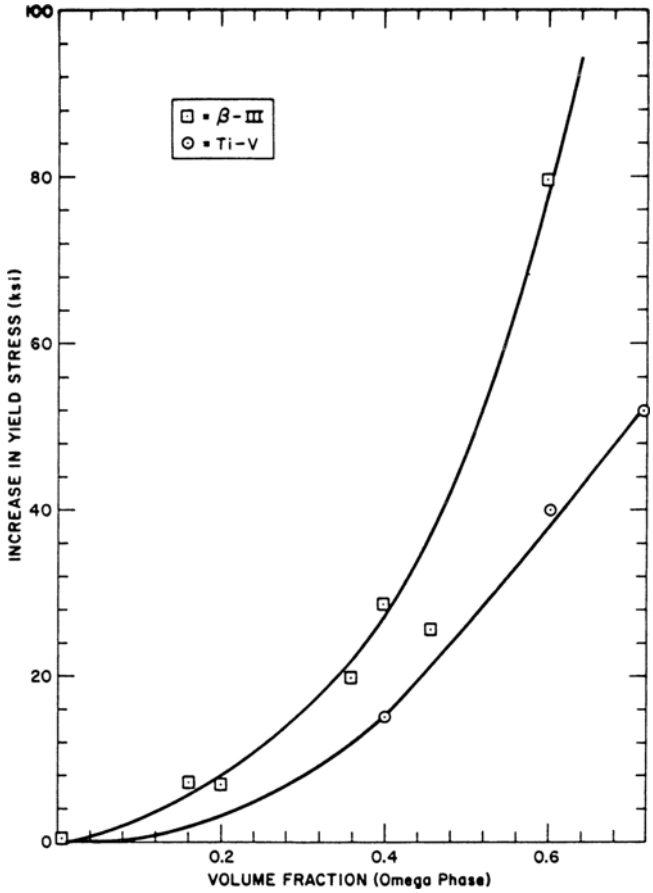

Fig. 8—Variation of yield strength with volume fraction of ω phase in Ti-V and β-III alloys.

formation mode has been established as slip at room temperature.

Finally, embrittlement of β-phase alloys by ω-phase formation will be considered. We have presented evidence which shows that the ω-phase particles are nondeformable and that even macroscopically brittle samples fail by a localized but ductile fracture mode, namely dimple rupture. Dimple rupture has been shown to occur by the nucleation, growth and coalescence of microvoids. Failure by this mechanism occurs at a critical strain, the critical strain being dictated by the material properties and state of stress. Koul and Breedis[11] have independently verified the dimple rupture fracture mode first reported by Williams, Boyer, and Blackburn.[8] They have attempted to analyze the fracture in terms of a critical stress criterion by invoking work hardening due to secondary slip around the ω particles. The critical stress concept is certainly useful in analyzing cleavage fracture, but the rationale for applying this concept to dimple rupture fracture in $\beta + \omega$ alloys is not clear. Further, as shown earlier, the work-hardening rate in Ti-Mo alloys is much lower than in Ti-V alloys, making a critical stress level even more difficult to achieve. It seems that a more reasonable explanation of the dimple rupture fracture would be based on the accumulation of a critical local strain for microvoid nucleation at β:ω interfaces since the ω-particles are nondeformable. The low work hardening rate in these alloys and the large number of voids which are nucleated, as evidenced by the small dimple size, result in a low resistance to necking and the sample can fail at extremely small and nonuniform strains.

We have demonstrated that the ω phase, if properly controlled, can be effective in the precipitation hardening of β-phase alloys. It should be noted that the composition and solution treatment temperature must be closely controlled to realize the maximum strengthening while avoiding embrittlement. Such controls may prove to be unrealistic in actual commercial practice and it is therefore questionable whether ω-phase strengthened alloys will ever be used. It may be possible to obtain a ternary or quaternary alloy in which the metastable equilibrium ω-phase volume fraction is $\sim$0.50 and in such a case ω-phase strengthening would appear to be practicable. No systematic attempt to produce such an alloy has been made at present and thus further work may be warranted in this area.

CONCLUSIONS

1) ω-phase strengthening of β-titanium alloys can be realized with reasonable ductility if the ω-phase volume fraction is less than 0.60.

2) Small amounts of ω phase, <25 pct volume fraction, have very little effect on either the strength or the ductility of the ω forming β-phase titanium alloys.

3) Embrittlement of β-phase alloys due to ω-phase formation is the result of microvoid nucleation, growth, and coalescence at very low macroscopic strains.

4) Thin film microscopy of deformed samples show that dislocations bypass the ω particles.

5) ω phase can be used in strengthening the β phase of an alloy low in beta stabilizing elements by first aging in the α-β region.

ACKNOWLEDGMENTS

The authors gratefully acknowledge the experimental assistance of D. H. Leslie, H. Nadler, P. Q. Sauers, R. A. Spurling, P. J. Stocker, and E. H. Wright.

REFERENCES

1. P. D. Frost, W. M. Parris, L. L. Hirsch, J. R. Doig, and C. M. Schwartz: *Trans. AMS*, 1954, vol. 46, p. 231.
2. B. S. Hickman: *J. Inst. Metals*, 1968, vol. 96, p. 330.
3. B. S. Hickman: *Trans. TMS–AIME*, 1969, vol. 245, p. 1331.
4. M. J. Blackburn and J. C. Williams: *Trans. TMS–AIME*, 1968, vol. 242, p. 2461.
5. J. C. Williams and M. J. Blackburn: *Trans. TMS–AIME*, 1969, vol. 245, p. 2352.
6. J. C. Williams, B. S. Hickman, and D. H. Leslie: *Met. Trans.*, 1971, vol. 2, p. 477.
7. J. M. Silcock: *Acta Met.*, 1958, vol. 6, p. 481.
8. J. C. Williams, R. R. Boyer, and M. J. Blackburn: *ASTM Spec. Tech. Publ.* 453, p. 215, ASTM, 1969.
9. M. J. Blackburn and J. C. Williams, *Trans. TMS–AIME*, 1967, vol. 239, p. 287.
10. M. J. Blackburn and J. A. Feeney: *J. Inst. Metals*, in press.
11. M. K. Koul and J. F. Breedis, *Met. Trans.*, 1970, vol. 1, p. 1451.